# Modeling Implementation of Smart Materials such as Shape Memory Alloys and Electro-Active Metamaterials

*M. Collet**

*Femto-ST Institute UMR CNRS 6174 Dept Applied Mechanics, Besançon, France*
*\*Corresponding author: 23 chemin de l'Epitaphe 25000 Besançon, manuel.collet@univ-fcomte.fr*

bang

**Abstract:** his paper aims at showing, through the description of two specific examples, how we can introduce smart material coupling effects by using Comsol Multiphysics® software and how electromechanical modeling reduction can be addressed for connecting the designed transducers as a substructure in a more complex system. The first example deals with dynamics modeling of non linear Shape Memory Alloy structure for structural shape control or semi-active damping optimization. The second example is dedicated to the electromechanical modeling of piezocomposite materials with their electronics shunts for their used to optimize vibroacoustical energy diffusion in complex mechanical systems.

**Keywords:** Smart Materials and Structures, Metamaterials Piezoelectric, Shape Memory Alloy

## 1 Introduction

The research activities in the fields of smart materials and structures today are very important and represent a large potential for the technological innovation in mechanics and electronics. The next generation of smart system will be constituted of active transducers and their driving electronics directly integrated in otherwise passive structures. A large research effort is now devoted for modeling smart materials and their multi-physical coupling effects in order to provide efficient numerical tools for robust optimization of this integrated adaptive composite structures constituted of a dense set of electro active cells. In this context Comsol Multiphysics® software appears as a very powerful and versatile numerical tool for finite element modeling of such smart behavior coupling many different physics such as thermal, mechanical or electro-magnetic phenomena. This paper aims at showing, through the description of two specific examples, how we can introduce such coupling effects by using Comsol Multiphysics® software and how electromechanical modeling reduction can be addressed for connecting the designed transducers as a substructure in a more complex system. The first example deals with dynamics modeling of non linear Shape Memory Alloy structure for structural shape control or semi-active damping optimization. The second example is dedicated to the electromechanical modeling of piezocomposite materials with their electronics shunts for their used to optimize vibroacoustical energy diffusion in complex mechanical systems.

## 1.1 Transient Dynamical response computation of Shape Memory Alloy materials and structures

## 2 Introduction

Shape Memory Alloy (SMA) are widely studied as an interesting smart material to actuate mechanical structures but also for its capability for inducing damping effect. Its use to optimize vibroacoustics responses involves a precise modeling of its dynamical behavior. The phase transformation between mother phase, the Austenite, and the induced one, the Martensite, leads to a strong non linear pseudo-elastic material behavior. The dissipated energy per hysteretic cycle can also be optimized to improve damping and/or isolation performance of the studied mechanical system [8, 6, 11]. The modeling approach involves the mul-

tiphysical description of the whole thermo-mechanical coupling especially when the dynamics response cannot be considered nor adiabatic nor isothermal. The part describes the developed numerical methodology to implement this behavior into Comsol® software for impact response computation.

## 3 Mathematical Formulation

Let us consider an open domain $\Omega$ bounded by a closed surface $\Gamma = \Gamma_u \cup \Gamma_t$ such as described in figure 1. $\vec{n}$ represents the outgoing normal vector to this surface.
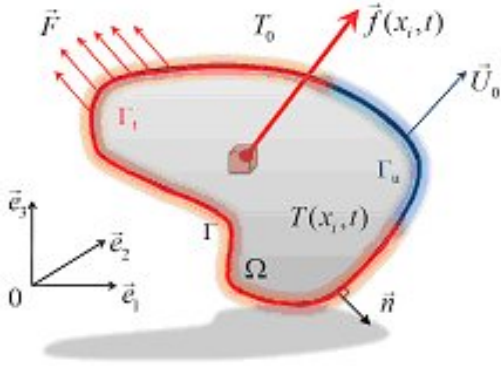


Figure 1: The considered mechanical problem and boundary conditions

The applied mechanical loads are : $\vec{U}_o$ the applied Dirichlet boundary conditions onto $\Gamma_u$; $\vec{F}$ the applied Neumann boundary conditions onto $\Gamma$ and $\vec{f}(x,t)$ the load inside the domain $\Omega$. In parallel the convection thermal boundary condition is introduced such as $\frac{\partial T}{\partial n} = \frac{h_o}{\lambda}(T - T_o)$ on $\Gamma$, where $T_o$ is the external temperature, $\lambda$ the thermal conductivity and $h_o$ the convection parameter. According to the Raniecki-Lexcellent model, widely described in [2, 8, 6, 11], on can show that the whole thermo mechanical equilibrium, without any internal thermal source term, can be written as in 1.

$$
\begin{aligned}
\rho\ddot{U}(x,t) - \nabla\underline{\sigma(x,t)} = f(x,t) & \quad \forall x \in \Omega \\
\rho C_v \dot{T}(x,t) + \nabla q = & \\
\theta^f(\bar{\epsilon},\xi,T)\dot{\xi}(x,t) - \alpha T(x,t)\underline{\sigma}:\underline{I} & \quad \forall x \in \Omega \\
\dot{\xi}\pi^f \geq 0 & \quad \forall x \in \Omega \\
\sigma.n = F(x,t) & \quad \forall x \in \Gamma_t \\
U = U_o(x,t) & \quad \forall x \in \Gamma_u \\
q.n = -h_o(T(x,t) - T_o) & \quad \forall x \in \Gamma
\end{aligned}
$$
(1)

where :

- $\sigma(x,t)$ and $\epsilon(x,t) = \frac{1}{2}(U.\nabla^T + \nabla U^T)$ stand for the Green-Lagrange constraints tensor and the associated Cauchy strain tensor, $\bar{\epsilon}$ being the equivalent Von Mises strain (i.e $\bar{\epsilon} = \sqrt{\frac{2}{3}dev(\underline{\epsilon}):dev(\underline{\epsilon})}$;

- $q$ is the thermal flow vector;

- $\xi$ is the induced Martensite fraction and $\pi^f$ the associated thermodynamical force such as : $\pi^f = 3\mu\frac{\gamma}{\rho}\bar{\epsilon} - (1 - 2\xi)\phi_{it}(T) - 3\frac{\mu}{\rho}\gamma^2\xi + \pi_o^f(T)$ where $\mu$ is one of the material Lame coefficient, $\gamma$ the maximum induced strain, $\phi_{it}(T)$ an affine function of temperature (see [2, 8, 6, 11] for definition);

- and $\theta^f = \pi^f + T\Delta s_o - (1-2\xi)\bar{s}_o$ where $s_o$ and $\bar{s}_o$ are entropy characteristic parameter inherent to the RL model (see [2, 8, 6, 11] for details);

- and $C_v$, $\alpha$ and $\rho$ respectively the material thermal capacity, the thermal expansion coefficient and the mass density.

The third inequality in 1 is direclty linked with expression of the second thermodynamical principle and stipulates inequality that must verify $\xi$ and its dual force $\pi^f$, that is to say, appears as a mathematical constraint for the constitutive model definition.

To close the mathematic problem defined in 1 we need to add all the behavior's relationships linking the primal unknowns $(\epsilon(U), \xi, T)$ to the associated dual forces given by the set of variables $(\underline{\sigma}, \pi^f, q)$.

The mechanical behavior equation is

$$
\underline{\sigma} = \underline{\underline{L}}(\underline{\epsilon} - \gamma\underline{K}\xi + \alpha(T - T_o)) \qquad (2)
$$

where $\underline{\underline{L}}$ is the Hook elasticity tensor and $\underline{K} = \frac{dev(\underline{\epsilon})}{\bar{\epsilon}}$ the tensor of phase induced strain direction. The thermal behavior relationship is simply given by the Fourier law such as

$$
q = -\lambda\nabla T \qquad (3)
$$

The most difficult relation to introduce, in this model, is really the constitutive equation linking the Martensite fraction $\xi$ to the others variables and that obey to the inequality constraint given in 1. The Raniecki-Lexcellent model define this relation such as

:

$$\xi \quad \in \quad ]0,1[ \qquad\qquad (4)$$

$$\dot{\xi} \quad = \quad \frac{3\mu\gamma\dot{\bar{\epsilon}} - \rho\Delta s_o \dot{T}}{\rho(\frac{A_1}{1-\xi} - 2\phi_{it}(T)) + 3\mu\gamma^3}.(\pi^f \geq 0).(\dot{\bar{\sigma}} > 0)$$

$$+ \frac{3\mu\gamma\dot{\bar{\epsilon}} - \rho\Delta s_o \dot{T}}{\rho(\frac{A_2}{\xi} - 2\phi_{it}(T)) + 3\mu\gamma^3}.(\pi^f \leq 0).(\dot{\bar{\sigma}} < 0)$$

$$\dot{\xi} \quad = \quad g(\bar{\epsilon}, \pi^f, \xi) \qquad\qquad (5)$$

where $A_1$ and $A_2$ are model parameters that can be identified by experimental measurement. Equation 5 represents two 'stateflow' Differential Algebraic Equations (i.e DAE) modeling, respectively, the direct phase transformation Austenite to Martensite (A ← M) when boolean function$(\pi^f \geq 0).(\dot{\bar{\sigma}} > 0) = 1$ and the reverse one M ← A when boolean $(\pi^f \leq 0).(\dot{\bar{\sigma}} < 0) = 1$. The boolean function insures that inequality constraint in 1 is verified, so equation 5 can replace it in the problem formulation. This equation constitutes the real difficulty of the numerical implementation especially when transient dynamical simulation is computed. Indeed, 'static' implementation has already been realized and used for computing equivalent complex modulus for harmonics non linear response analysis [11, 6, 8]. This static computation allow us to describe stress-strain relationship with internal loop, as presented in figure 2, for complex mechanical system.
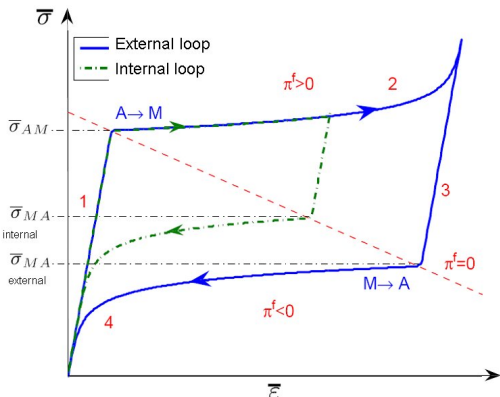


Figure 2: Static model capability : internal loops representation

# 4 Comsol[R] Transient Model Implementation and Numerical Results

The presented results here only concern isothermal implementation where temperature is considered as constant. The aim of this first step is only to study capability of the software to integrate non linear problem incorporating 'stateflow' Differential Algebraic Equations. In this context, the problem formulation is also given by

$$\begin{array}{ll} \rho\ddot{U}(x,t) - \underline{L}\nabla(\underline{\epsilon} - \gamma\underline{\underline{K}}\xi) = f(x,t) & \forall x \in \Omega \\ \dot{\xi} = g(\bar{\epsilon}, \pi^f, \xi) & \forall x \in \Omega \\ \sigma.n = F(x,t) & \forall x \in \Gamma_t \\ U = U_o(x,t) & \forall x \in \Gamma_u \end{array}$$

$$(6)$$

## 4.1 Comsol software[R] Implementation

The numerical implementation into Comsol software[R] is based on the resolution of a coupled problem between a weak formulation of first equation of (6) and a Equation-Based modeling of the second equation. Each boolean operator used in the formulation has been replaced by smoothed Heaviside function with continuous first derivative *flsc1hs* in Comsol. An implicit time-stepping scheme is used for the time-dependent solver algorithm, based on DASPK solver [4] (variable-order and variable-stepsize backward differentiation). The nonlinear system of equations at each time step is solved using a Newton-Raphson scheme. The tangent unsymmetric sparse linear system is finally solved using direct UMFPACK solver [1].

In the context of transient dynamics, such as responses to impacts, some numerical tests have shown that the convergence of the solvers was quite bad, inducing very large computation times or even not converged results. One of the main reasons for this is undoubtely the strong nonlinearity of the kinetic law 5. Trying to impose those expressions directly leads to very small time steps or algorithms stops. The way which has been chosen in this case for smoothing the numerical difficulties induced by the kinetic law, is to add an inertial term in it, which can be justified both numerically and physically:

- In a numerical point of view, the inertial terms will smooth the equation,

changing it from a first order to a second order one.

- In a physical point of view, the austenite to martensite transformation is not instantaneous, and it has been observed that the speed of transformation is linked to the speed of sound in the alloy. This term could have a significant impact when structural solicitations induce speeds which are comparable to the sound velocity, while being negligible for quasi-static or "low-frequency range" applications.

The kinetic law 5 has then been modified to :

$$t_m \ddot{\xi} + \dot{\xi} = f(\sigma_{vm}, \pi_f, \xi) \tag{7}$$

in which $t_m$ is a parameter which can be chosen depending on the speed of sound in the alloy, it is homogeneous to a relaxation time.
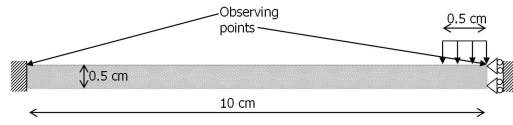
## 4.2 Numerical results



Figure 3: Boundary Conditions and Mesh of the 2D-structure

The structure which has been used in the numerical simulations is a 2D plane stress component, shown on figure 3. Its dimensions are 0.5 cm by 10 cm, and the beam is clamped in $x = 0$ and vertically guided in $x = 0.1$m. Two observing points are shown on the figure. The mesh has 2048 quadratic TRI6 elements for the mechanical solver and 2048 linear TRI3 elements for the martensite rate distribution solver, resulting in a total of 19115 degrees of freedom (displacement for the structure and martensite rate).

The impact force is applied on the upper part of the beam as shown on figure 3, during 1ms. The composition of the SMA used in the numerical applications is $CuAlBe$. Its characteristic phase transformation temperatures measured by electrical resistance evolution are : $M_f^0 = 191K$, $M_S^0 = 213K$, $A_S^0 = 205K$, $A_F^0 = 221K$. The material Parameters are : $E = 7.5 \cdot 10^{10} Pa$, $\rho = 8129 kg \cdot m^{-3}$, $\Delta u^* = 2871.6 J \cdot m^{-3}$, $\Delta s^* = 11 J \cdot m^{-3}$, $u_0 = 100.3 J \cdot m^{-3}$, $\gamma = 0.0295$, $\alpha = 0.055$, $Cv = 490 J \cdot kg^{-1}$,

$\alpha_0 = 17 \cdot 10^{-6} K^{-1}$.

As a first observation from the numerical tests, one can observe that the phase transformation has a significant effect on the global damping. On figure 4, two results are shown : the first one is related to the SMA calculation corresponding to the above description, and the second one corresponding to a linear equivalent material (same resolution, with an imposed zero martensite rate). The curve shows the vertical displacement of observing point, and one can clearly observe that the SMA decrease is faster than the linear one. The time response of the linear model has a frequency of 360 Hz associated to a damping ratio of 0.11, while the time response of the SMA model has a frequency of 243 Hz and a damping ratio of 0.24.
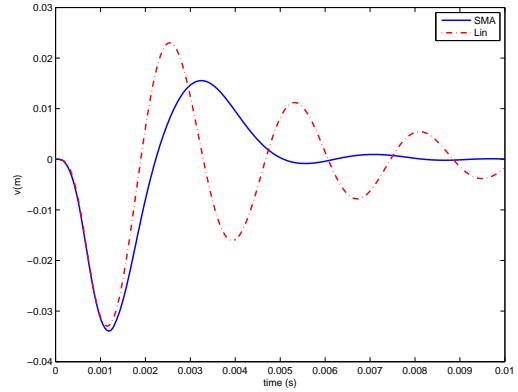


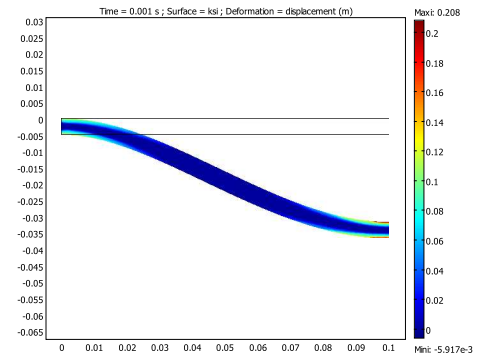Figure 4: Vertical displacement of observing point, comparison SMA/Lin



Figure 5: Martensite rate distribution at t = 1 ms (end of impact)

On figure 5, one can observe the spatial displacement of the structure, and the martensite rate at time of impact end. The martensite rate has a maximal value on the zones

in which the stress is maximal. One can observe on figures 6 and 7 evolution of $\xi$ and $\pi^f$ : while the thermodynamic force is negative, the martensite rate has a constant zero value. As soon as the force becomes positive, the rate increases, until the force becomes negative, because up to 1 ms, the time derivative of the Von Mises Stress is always positive. So before 1 ms, each sign change of the thermodynamic force induces a inflexion in the curve of the martensite rate.
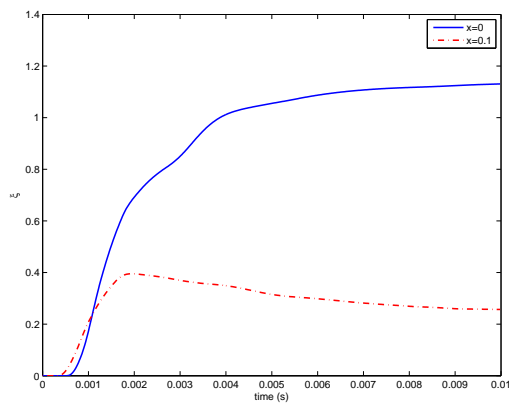


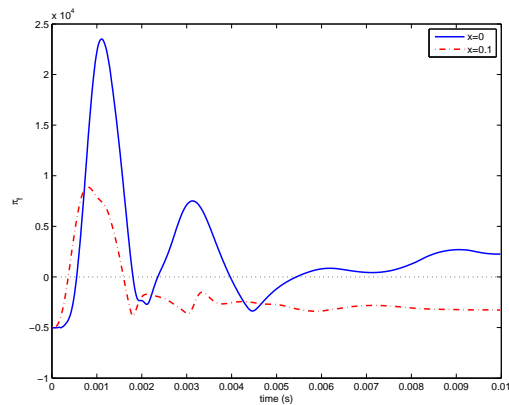Figure 6: Time evolution of martensite rate at observing points



Figure 7: Time evolution of thermodynamic force

One can also observe on figure 6 that the model has a physical incoherence, since the maximum martensite rate is above 1 (about 1.12), which has no physical meaning. This particular point is undoubtely a critical point in the model and will be of importance in the future works where bounded constraints on $\xi$ evolution will be explicitly introduced in the modeling approach. A real effort will also be made to regularize the 'stateflow' DAE and improve convergence for high speed response computation.

# 5  Modal Synthesis and Dynamical Condensation Methods for Accurate Piezoelectric Systems Impedance Computation

Now days, Piezoelectric transducers are widely used in many physical and industrial applications. Optimization of their behavior is of major interest for smart system design. In current practice, smart structure integration involves a broad multiphysical modeling approach including mechanics, smart materials, coupling effects and electronics implementation. When global energy optimization is considered, all coupling mechanisms should be carefully introduced in the simplest possible modeling procedure. For piezoelectric material these constraints involve the construction of a robust model (simple and precise) able to represent the piezoelectric coupling, or from another perspective, to correctly implement piezoelectric electromechanical impedances. This latter perspective enables the optimization and design of electronic devices connected to the piezoelectric material. The objective of this part is to present a model reduction approach that yields a piezoelectric super element guaranteeing accurate computation of a piezoelectric transducer's mechanically coupled electrical impedance.

This part presents a short sum up of the developed approach for condensing piezoelectric model previously published in [7]. We propose, here, a new, simple and efficient approach for piezoelectric condensation implemented by using Comsol Multiphysics®. This allows the electronic coupling to be fully used in the optimization of passive shunted piezoelectric transducers, energy harvesting piezoelectric systems or dense distributed transducers. The obtained model through this approach is also versatile, of small size, and is therefore quite tractable for use in intensive computation algorithms.

## 5.1 Theoretical Model Synthesis for substructuring approach

Let us consider a generic piezo-mechanical transducer connected to an external complex mechanical system through interfaces. In order to take into account the piezoelectric induced voltage field, fundamental to precisely describe piezoelectric coupling behavior (as demonstrated in [3]), we use a 3D Finite element description of the complete system. Introducing all set of boundary conditions, one obtain the standard set of ordinary differential equation :

$$
\begin{bmatrix}
M_{ii} & M_{ic} & 0 & 0 \\
M_{ic}^T & M_{cc} & 0 & 0 \\
0 & 0 & 0 & 0 \\
0 & 0 & 0 & 0
\end{bmatrix}
\begin{bmatrix}
\ddot{w}_i \\
\ddot{w}_c \\
\ddot{V} \\
\ddot{V}_p
\end{bmatrix} +
$$

$$
\begin{bmatrix}
K_{ii} & K_{ic} & E_i & E_{ip} \\
K_{ic}^T & K_{cc} & E_c & E_{cp} \\
-E_i^T & -E_c^T & C & C_p \\
-E_{ip}^T & -E_{cp}^T & C_{cp}^T & C_{pp}
\end{bmatrix}
\begin{bmatrix}
w_i \\
w_c \\
V \\
V_p
\end{bmatrix} =
$$

$$
\begin{bmatrix}
f + T_o \\
\sum_{i\in[1..I]} T_{u_i}^s \\
0 \\
Q_p
\end{bmatrix}
$$

$$
w_{sc} - w_c = 0
$$

$$(8)$$

The transducer degrees of freedom are split as $w_i$ for the inner part and $w_c$ for the connecting part of the displacement. Partition of the voltage terms is introduced by using $V$ for unknown voltage degrees of freedom and $V_p$ for the applied piezoelectric potential. The output equation for each electrode $S_{vq}^p$ is the last line of the matrix equation in (8).

The proposed condensation method is based on using the static Schur complement [5] of the stiffness matrix obtained in equation (8).This approach has been used in previous work [5, 12, 13] to reduce the number of piezoelectric degrees of freedom for large system computation.

First, one consider the Schur complement applied to the piezoelectric set of equations (8). As equation (8) indicates, the electrical behavior response of such a system is essentially static. In fact, by simply introducing the Schur complement of the first $3\times3$ bloc of the stiffness matrix $K$, one obtain a new expression of the dynamical equilibrium of our piezoelectric system. Secondly, by introducing the matrix product $\begin{bmatrix} -C^{-1}C_p \\ I \end{bmatrix} V_p =$

$\begin{bmatrix} \bar{V}_p^o \\ I \end{bmatrix} V_p = V_p^o V_p$ gathering all the static dielectric solutions,for each different applied voltages and by adopting a simplified bloc matrix notation, equation (8) can be rewritten as:

$$
M\ddot{w} + (K + EC^{-1}E^T)w = -E_p^o.V_p^o.V_p + F + T
$$
$$
-E^T.w + C\bar{V} = -\bar{C}_p^o.V_p^o.V_p
$$

$$(9)$$

$$
Q_p = -V_p^{oT}E_p^{oT}w + C_p^o V_p \qquad (10)
$$

where $F$ and $T$ stands for the external disturbing forces and the connection reactions, $\bar{V} = V - \bar{V}_p^o V_p$ is the induced electrical potential, $w = \begin{bmatrix} w_i \\ w_c \end{bmatrix}$, $E_p^o = \begin{bmatrix} E_i & E_{ip} \\ E_c & E_{cp} \end{bmatrix}$, $E = \begin{bmatrix} E_i \\ E_c \end{bmatrix}$, $\bar{C}_p^o = \begin{bmatrix} C & C_p \end{bmatrix}$, and $M$ and $K$ are respectively the first $2 \times 2$ bloc of the mass and stiffness matrices in equation (??). We also introduce the equivalent piezoelectric capacity (for zero displacement) $C_p^o = C_{pp} - C_p^T C^{-1} C_p$.

The direct use of Craig and Bampton methods to condense such piezoelectric coupled system in (8) would introduce a full mass matrix, coupling the electrical voltage degrees of freedom to the other generalized coordinates. Thus, we would use a second electrical inputs term $\ddot{V}_p$ which is not intrinsically a desirable approach.

The key novelty of our proposed method is to add the dual static displacement field adjoint to the imposed piezoelectric force $-E_p^o.V_p^o$ in (9) to the original Craig and Bampton basis. Therefore, the proposed approximation basis may be represented as 3 sets of displacement fields:

1. The classical static Craig and Bampton displacement field corresponding to the static solutions of the unitary non-homogeneous Dirichlet imposed connecting conditions. These fields are constrained to be orthogonal to the applied piezoelectric force. The solutions $W_u = \begin{bmatrix} \left\{ \begin{matrix} w_{u_i} \\ V_{u_i} \end{matrix} \right\}_{\forall i} \end{bmatrix}$ are also solutions of the generic mechanical problem

$$
(K + EC^{-1}E^T)w_{u_i} = 0
$$
$$
-E^T.w_{u_i} + CV_{u_i} = 0
$$
$$
B_u(i,:)w_{u_i} = 1
$$
$$
-w_{u_i}^T E_p^o V_p^o = 0
$$

$$(11)$$

where $B_u$ represents the localization boolean matrix of the connecting degrees of freedom such as for each $i$ designating a particular connecting degree of freedom $B_u(i,:)w = w_c(i) = 1$, where $B_u(i,:)$ is the $i^{th}$ row of $B_u$.

2. A set of the dual displacement fields adjoint to the piezoelectric applied forces computed with homogeneous connecting Dirichlet condition. These displacements $W_{v_p} = \left\{ \begin{bmatrix} w_{v_p} \\ V_{v_p} \end{bmatrix} \right\}_{\forall p}$ are solutions of the generic mechanical problem

$$
\begin{aligned}
&(K + EC^{-1}E^T)w_{v_p} = 0 \\
&-E^T w_{v_p} + CV_{v_p} = 0 \\
&B_u w_{v_p} = 0 \\
&-w_{v_p}^T E_p^o V_p^o(:,p) = 1
\end{aligned} \quad (12)
$$

for each $p$ applied unitary static potential vector $V_p^o(:,p)$ ($V_p^o(:,p)$ represents the $p^{th}$ column of the static dielectric solutions matrix $V_p^o$).

3. A set of fields that are the inner normal modes with homogeneous Dirichlet connecting conditions, orthogonal to the piezoelectric applied forces. These $N$ fields are represented as $\Phi_N = \left[ \left\{ \begin{array}{c} \phi_n \\ V_{\phi_n} \end{array} \right\}_{\forall n} \right]$ and are the first $N$ solutions of the eigenvalue problem represented by

$$
\begin{aligned}
&(-\omega_n^2 M + (K + EC^{-1}E^T))\phi_n = 0 \\
&-E^T \phi_n + CV_{\phi_n} = 0 \\
&B_u \phi_n = 0 \\
&-\phi_n^T \begin{bmatrix} E & E_p \end{bmatrix} V_p^o = 0
\end{aligned}
$$
$$(13)$$

The number of degrees of freedom in equations (8) can also be reduced by simply assuming serial truncation. By using the classical covariant transformation, Equations (8) can be reduced to

$$
\begin{bmatrix} M_{cc} & M_{cp} & M_{cn} \\ M_{cp}^T & M_{pp} & M_{pn} \\ M_{cn}^T & M_{pn}^T & I_N \end{bmatrix} \begin{bmatrix} \ddot{w}_c \\ \ddot{\eta}_p \\ \ddot{\eta}_n \end{bmatrix} +
$$
$$
\begin{bmatrix} K_{cc} & K_{cp} & 0 \\ K_{cp}^T & K_{pp} & 0 \\ 0 & 0 & \Omega_N^2 \end{bmatrix} \begin{bmatrix} w_c \\ \eta_p \\ \eta_n \end{bmatrix} =
$$
$$
\begin{bmatrix} \sum_{i \in [1..I]} T_{u_i}^s \\ 0 \\ 0 \end{bmatrix} + \begin{bmatrix} 0 \\ I_p \\ 0 \end{bmatrix} .V_p + F + T_o
$$
$$
w_{sc} - w_c = 0
$$
$$(14)$$

and

$$
q_p = \begin{bmatrix} 0 & I_p & 0 \end{bmatrix} \begin{bmatrix} w_c \\ \eta_p \\ \eta_n \end{bmatrix} + C_p^o V_p \quad (15)
$$

where $I_N$ stands for the $N$ order unitary matrix, $\Omega_N$ for the diagonal matrix of the eigenvalues $\omega_n$ solutions of (12), and $F$ and $T$ are the projection of the exterior applied forces onto the basis.

## 5.2 Comsol Multiphysics® Implementation for Modeling of a Piezostack Transducer

### 5.2.1 System overview

The structure of interest is depicted in figure 8. It is a 2D plane stress state model of a beam element (substructure 2) connected to an active substructure containing a piezostack transducer. The ends of the beam are assumed to be clamped. The main aim of our computation is to furnish an accurate piezoelectric super element of the active substructure by using the methodology developed above. The final assembled system should exhibit the same static and dynamic behavior as a directly meshed structure and therefore the same impedance.
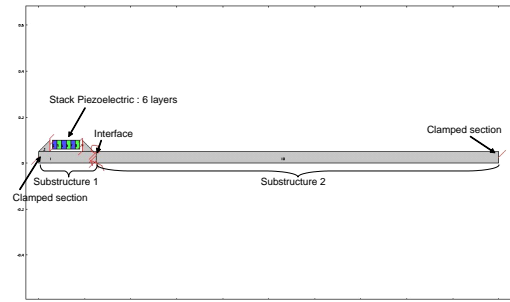


Figure 8: Mechanical system overview, indicating substructuring between piezoelectric section and passive section

The active substructure (substructure 1 in figure 8) is more precisely depicted in figure 9. The mechanical characteristics are steel for the beam and classical PZT(P1.91) for the piezostack.
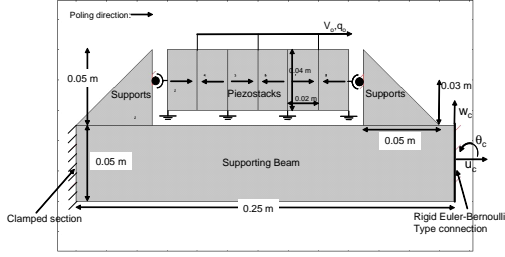
Figure 9: Details of Active Substructure

The mechanical boundary conditions indicated in figure 9 are clamped on the left end and "Bernoulli Euler" kinematic fields on the right-hand interface. On this right-hand interface, the 2D displacements $u_i(y,t)$ and $w_i(y,t)$, respectively along axis $Ox$ and $Oy$, are given so that $u_i(y,t) = u_i^o(t) - (y - \frac{l_r}{2})\theta_i^o(t)$ and $w_i(y,t) = w_i^o(t)$ where $l_r$ represents the section height.

The electrical boundary conditions are also depicted in figure 9. The lateral edges of each stack layer are free of electrical charge. The connecting stack interfaces are alternatively grounded and subjected to an applied common electrical potential $V_p$. The piezostack component is connected to the support at the center of its left- and right-hand face to simulate a ball joint.

The initial mesh has 1312 Lagrange Quadratic triangle elements with four Gauss points per element. The initial total number of degrees of freedom to mesh this part is 7182. Mesh cases 2 has 20490 degrees of freedom for modeling the active part and Meash case 3 refines the passive mesh density by adding 3778 degrees of freedom. After condensation the active substructure has always 9 generalized degrees of freedom.

## 5.3 Remarks on Comsol Multiphysic® software implementation

Comsol Multiphysic® software is used for implementing the model. The necessary implementation of non-classical Dirichlet constraints, as in equations (11), (12) and (13), may be directly introduced using this software platform. The piezoelectric dual constraint is introduced as a sub-domain integral constraint. Integrations are carried out

in each piezoelectric sub-domain by using an electro-static field $V_p^o$ (here $p = 1$) obtained by solving equation (??), as indicated by

$$DualConst = \int_{\Omega_p} -e^T \nabla V_p^o \nabla_{sym}\delta w d\Omega \tag{16}$$

This is introduced in Comsol Multiphysic® software by using Subdomain Integration Variables such as :

```
Vs1x='-e33_smppn*Ex_es/S'
Vs1y='-e31_smppn*Ex_es/S'
Vs1xy='-e15_smppn*Ey_es/S'
Vcont1='-thickness_smppn*...
   (Vs1x*ex_smppn+Vs1y*ey_smppn+...
   2*Vs1xy*exy_smppn)'}};
```

these terms being added as a Point Constraint to be set to 0 as in equation (11) and (13) or to 1 as in equation (12) depending on each step of the computations as presented above. The global assempbling is made of successive computation with Comsol Multiphysic®. Initially we compute the electro-static field $V_p^o$ by solving in piezo-electric domains electrostatic problem with the corresponding permittivity data. So, static and eigenvalue problem are solved by setting constant to imposed connecting and the dual constraints (16). The connecting fields are obtained by imposing successively each interface degrees of freedom (i.e here Ux,Uy,Rotz) to 1 and dual constraint (i.e : Vcont1) to 0

```
% Constants
fem.const = {'Vin','1', ...
   'Rotz','0', ...
   'Ux','1', ...
   'Uy','0', ...
   'Vcont1','0'};
```

or for dual piezoelectric field , $Vcont1 = 1$ and the other constant are 0. The eigenvalue problem are solved with all constant equal to 0.

The assembling super element is made by projecting the initial problem onto these computed basis. Each term are obtained by using 'postint' command on a complex assembled fields made of each pair of basis vectors:

```
femTot.sol=femsol(femMod.sol.u(:,ii)+...
i*(femMod.sol.u(:,jj)));
```

```
M(ii,jj)=postint(femTot,...
'rho_smpn*thickness_smpn*...
(real(u)*imag(u)+real(v)*imag(v))',...

K(ii,jj)=(postint(femTot,'thickness_smpn*...
(imag(ex_smpn)*real(sx_smpn)+...
imag(ey_smpn)*real(sy_smpn)+...
2*imag(exy_smpn)*real(sxy_smpn))',...
```

## 5.4 Obtained Results

The main interest of the proposed method is the ability to compute the global piezoelectric response functions by taking into account the global behavior of such a system. To demonstrate this capability, figure 10 depicts the frequency response function of the piezoelectric charge for a unit voltage input, $\frac{q_p(\omega)}{V_p(\omega)}$. Results for the four mesh cases are shown: the global mesh (direct computation), and refined mesh 1, 2 and 3. The figure does not reveal any "visual" difference between the results. We note the well-known closed poles/zeros location of the electric transfer function for a piezoelectric system. The capability to compute these quantities are fundamental for optimizing active or passive control systems that use such a piezoelectric transducer[9, 10].
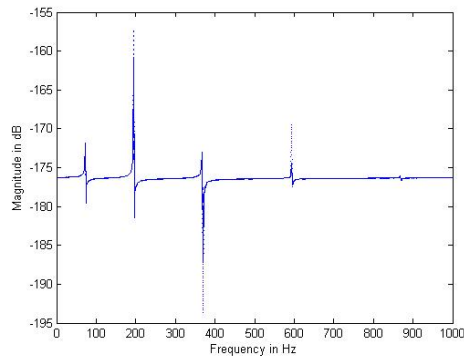


Figure 10: FRF $\frac{q_p(\omega)}{V_p(\omega)}$ for the global mesh (dotted line), refined mesh 1 (dash line), 2 (dashdot line) and 3 (plain line)

The five first poles (resonance frequencies) and zeros (antiresonance frequencies) of the electrical transfer function $\frac{q_p(\omega)}{V_p(\omega)}$ are very closed that confirm accuracy of our proposed approach. Notice that the substructuring approach results are precise enough to compute poles and zeros location with a maximum error, here, of about 0.2 % with the initial mesh. The convergence of the method is clearly indicated by this set of numerical tests.

## 6 Conclusion

Through the description of two examples, we underline, on this paper, the need of efficient and versatile tools for numerical simulation of linear or non linear multiphysics system when new type of smart structure is studied. Our developed approaches aims at building rapid and dedicated model of smart material interaction for intensive mechanical optimization computation. This problem need conjunction of physical analysis and modeling, clever problem formulation and dedicated numerical tools for solving (including condensation techniques). The used of Comsol Multiphysic® software allows us to efficiently play with problem formulation in an open software easy to use. Numerical solving can also be done by directly using Comsol's toolbox but, also, by implementing our own approach. Interface with Matlab (or Comsol Script®) allow us to develop our own numerical model on a generic applied mathematic platform where many complementary numerical tools are provided ('home made' softwares, open toolbox...). This is a crucial point for the success of our future smart system development.

## References

[1] Davis T. A., *Algorithm 832: Umfpack v4.3, an unsymmetric-pattern multifrontal method*, ACM Transactions on Mathematical Software **30** (1994).

[2] K. Tanaka B. Raniecki, C. Lexcellent, *Thermomechanical models of pseudoelastic behaviour of shape memory alloys.*, Archives Mech. **3** (1992), 261–284.

[3] A. Benjeddou, *Advances in piezoelectric finite element modeling of adaptive structural elements : a survey*, Computers and Structures **76** (2000), 347–363.

[4] Petzold L. R. Brown P. N., Hindmarsh A. C., *Using krylov methods in the solution of large-scale differential-algebraic systems*, SIAM Journal on Scientific Computing **15** (1994), 1467–1488.

[5] C. Haenel M. Bernadou, *Modelisation and numerical approximation of piezoelectric thin shell. part ii : Approximation by finite element methods and numerical experiments*, Comput. Method. Appl. Mech. Engrg. **192** (2003), 4045–4073.

[6] C. Lexcellent M. Collet, E. Foltète, *Analysis of the behavior of a shape memory alloy beam under dynamical loading*, Eur. J. of Mechanics: A. Solids **20** (2000), 615–630.

[7] K.A Cunefare M Collet, *Modal synthesis and dynamical condensation methods for accurate piezoelectric systems impedance computation*, Journal of Intelligent Material Systems and Structures (2008).

[8] L. Heller C Lexcellent M Collet, E Foltête, *Non linear dynamic behavior of shape memory alloy*, Smart Structures and Materials (Active Materials: Behavior and Mechanics), SPIE, 2004, pp. 210–218.

[9] M. Collet P. Monnier, *Definition of the mechanical design parameters to optimize efficiency of integraol force feedback active damping strategy*, Journal Structural Control and Health Monitoring **12** (2005), 65–89.

[10] A. Preumont, *Vibration control of structures : An introduction*, Kluwer, 1997.

[11] Collet M. Foltete E. Thiebaud F., Lexcellent C., (2007).

[12] V.K. Varadan V.V. Varadan, Y.H Lim, *Closed loop finite-element modeling of active/passive damping in structural vibration control*, Smart Materials and Structures **5** (1996), 685–694.

[13] S.Y. Wang, *A finite element model for the static and dynamic analysis of piezoelectric bimorph*, Int Journal of Solid and Structures **41** (2004), 4075–4096.